Available online at www.sciencedirect.com
ScienceDirect
Ocean Engineering 33 (2006) 2195–2208
OCEAN ENGINEERING
www.elsevier.com/locate/oceaneng

Mud mass transport due to waves based on an empirical rheology model featured by hysteresis loop

P. Qi*, Y.J. Hou

Institute of Oceanology, Chinese Academy of Sciences, Qingdao 266071, PR China

Received 20 January 2005; accepted 19 October 2005
Available online 3 March 2006

Abstract

A vertical 2-D water–mud numerical model is developed for estimating the rate of mud mass transport under wave action. A nonlinear semi-empirical rheology model featured by remarkable hysteresis loops in the relationships of the shear stress versus both the shear strain and the rate of shear strain of mud is applied to this water–mud model. A logarithmic grid in the vertical direction is employed for numerical treatment, which increases the resolution of the flow in the neighborhood of both sides of the interface. Model verifications are given through comparisons between the calculated and the measured mud mass transport velocities as well as wave height changes.

Keywords: Mud mass transport; Wave attenuation; Soft mud bed; Rheology model; Hysteresis loop; Water waves; Muddy coasts

1. Introduction

Muddy coasts covered with very soft fine sediments or underconsolidated clays are usually found at the mouths of major rivers, such as the Mississippi, Amazon, Niger, Ganges-Brahmaputra, Mekong, and Yellow. Almost all these river mouths are the

*Corresponding author. Fax: +86 532 82898612.
E-mail address: pqi@ms.qdio.ac.cn (P. Qi).

0029-8018/$ - see front matter
doi:10.1016/j.oceaneng.2005.10.021

Nomenclature

a	amplitude of η
d	depth of water layer or mud layer
G_0	parameter of rheology model
H	surface wave height
n	complex wave number
p	dynamic pressure
t	time
T	wave period
u	velocity component in x-direction
$\tilde{u}$	amplitude of velocity component u
$\tilde{w}$	amplitude of velocity component w
$\tilde{p}$	amplitude of pressure p
w	velocity component in z-direction
W	water content ratio
x	horizontal coordinate
z	vertical coordinate

Greek letters

α	parameter of rheology model
β	parameter of rheology model
μ_0	parameter of rheology model
η	free surface displacement
δ	wave attenuation rate
ξ	component of mud particle displacement in x-direction
ς	component of mud particle displacement in z-direction
τ	shear stress
ε	shear strain
$\varepsilon_{\max}$	maximum shear strain
γ	rate of shear strain
ρ	density of water or mud
v	viscosity of water or mud

Subscripts

0	initial values
E	Eulerian coordinate
l	equals 1 or 2
L	Lagrangian coordinate
m	mud layer
r	real part
w	water layer

main sea-going exists of important waterways. Many of these muddy coasts are the site of major activities related to the installation and operation of offshore oil and gas production platforms and pipelines (Kraft and Watkins, 1976).

In such areas, when water waves propagate over a seabed of soft mud, two noteworthy phenomena take place due to the interaction between the water body in wave motion and the mud bed. One is large mud mass transport and the other is high wave attenuation as the waves propagate over the mud bed. The significance of mud mass transport in the mud layer could be recognized in the field experiment in Kumamoto, Japan (Kihara et al., 1987). Regarding to the wave attenuation over mud beds, Gade (1958) notes that there is a location off the central Louisiana coast, known as the Mud Hole, where the wave attenuation due to the mud bed is so great that fishing boats use it as an emergency harbor during storms. The river mouth area of the Yellow is also known as “Mud Hole” in China.

The studies of water waves over mud beds have been conducted since the first work of Gade in 1958. Constitutive model characterizing mud dynamics becomes essential in formulating the problem of water waves over mud beds. For example, a viscous fluid model was used by Gade (1958) and Dalrymple and Liu (1978); an elastic model by Mallard and Dalrymple (1977) and Dawson (1978); a poro-elastic model by Yamamoto and Takahashi (1985); a visco-elastic model by Macpherson (1980); Hsiao and Shemdin (1980) and Maa and Mehta, (1990); a Bingham fluid model by Krone (1963) and Mei and Liu (1987). The experimental results by Trien et al. (1990) show the visco-elastic–plastic characteristics of mud under waves, that is the mud exhibits a nearly viscoelastic behavior at low shear rate, and a Bingham fluid behavior at hight shear rate. Mathematical modeling based on the visco-elastic–plastic model was presented by Shibayama et al. (1990) and Trien (1991). Recently, laboratory experiments were conducted for more than 800 runs by Jiang (1996) using the kaolinite soft mud under such oscillatory external forces as water waves. The mud showed combined features of viscous, elastic and plastic materials depending on the magnitude of external forces and especially on its water content ratio. The shear stress of the mud is a function of both the shear strain and the rate of shear strain with strong nonlinearity featured by remarkable hysteresis loops in their relationships. Although, this model is still not the final choice considering the complexity of mud rheological behavior, we use it in the present study to develop a relatively simple predictive model for wave–mud interaction problem.

In the present study, a two-layer water–mud model based on the nonlinear semi-empirical rheology model by Jiang (1996) is developed for water waves interaction with a soft mud bed and the resultant mud mass transport. The features of the proposed rheology model of soft mud by Jiang (1996) are further described in Section 2. By incorporating the proposed rheology model with the linearized Navier–Stokes equations, a vertical 2-D numerical model is then formulated in Section 3, followed by the description of boundary and initial conditions in Section 4. The mud mass transport velocity is formulated in Section 5. In Section 6, mud mass transport velocities as well as rates of the decay of the surface water wave heights are calculated and compared with the experimental data concerned.

2. A semi-empirical rheology model of the kaolinite soft mud under cyclic loadings

Rheology is defined as the study of relationships between "stress" and corresponding "strain" or "the rate of strain". Recently, the rheological response of soft mud to oscillatory forcing like waves was studied experimentally with a dynamic rotary shear viscometer (Jiang, 1996). From the experiments, it is concluded that the soft mud is characterized by the combined visco-elastic–plastic properties under such oscillatory external forces as water waves. The shear stress of the mud is a function of both the shear strain and the rate of shear strain with strong nonlinearity featured by remarkable hysteresis loops in their relationships. The constitution equation is generally written as

$$\tau = \frac{G_0 \varepsilon}{1 - \alpha|\varepsilon|} + \frac{\mu_0 \gamma}{1 + \beta|\gamma|} \tag{1}$$

in which, τ, ε and γ denote shear stress, shear strain and the rate of shear strain, respectively; G_0, μ_0, α and β are model parameters, G_0 denoting the initial shear modulus at $\varepsilon = 0$, μ_0 the initial viscosity at $\gamma = 0$, and α and β being coefficients determining the shapes of the backbone curves (Jiang, 1996).

The empirical expressions for these model parameters are as follows:

$$\begin{aligned} G_0 = {} & (5.56042 \times 10^5 \cdot W^{-2.76631}) \cdot \{[-7.25526 - 558.83242 \\ & \cdot (1 + \tanh(-0.57846 \cdot T))] + [81.69310 + 707.43501 \\ & \cdot (1.0 - \tanh(-0.47194 \cdot T)) \cdot \alpha^{\frac{1.714}{\{1.0+9.872 \cdot \exp(-0.866 \cdot T)\}}}\}, \end{aligned} \tag{2}$$

$$\begin{aligned} \mu_0 = {} & \{5.56042 \times 10^5 \cdot W^{-2.76631}\} \cdot \{29.0336 \cdot (1.31^{\mathrm{T}})\} \\ & \cdot \ln\{[24.714 \cdot \exp(-0.308 \cdot T)] \cdot \beta + 1.0\}, \end{aligned} \tag{3}$$

$$\begin{aligned} \alpha = {} & \frac{1}{\varepsilon_{\max}} \{1.0 - (0.79051 - 5.04571 \times 10^{-3} \cdot T) \\ & \cdot \exp(-[0.74946 \cdot \tanh(0.242983 \cdot T)] \cdot \varepsilon_{\max})\}, \end{aligned} \tag{4}$$

$$\beta = (0.34135 + 0.088222 \cdot T + 0.011651 \cdot T^2) \cdot \varepsilon_{\max}^{(1.04529 - 1.41946 \cdot T^{0.174215})}, \tag{5}$$

where $\varepsilon_{\max}$ is the maximum shear strain, T the period of cyclic shear loads, W the water content ratio.

The constitution equation, Eq. (1), and the formulas for the model parameters G_0, μ_0, α and β, Eqs. (2)–(5), form a complete rheology model for the soft mud under the action of cyclic loads. Fig. 1(a) and (b) show the calculated results of the shear stress versus the shear strain as well as the shear stress versus the rate of shear strain for the case in which the water content ratio is 200%, and the period of the cyclic load is 6.0 s. These figures are in good agreement with the measurements (see Jiang, 1996). We find that the stress-strain as well as the stress-rate of strain paths form hysteresis loop instead of a single curve. We also discover that the stress-strain path is nearer to linear if the strain is small. Otherwise,

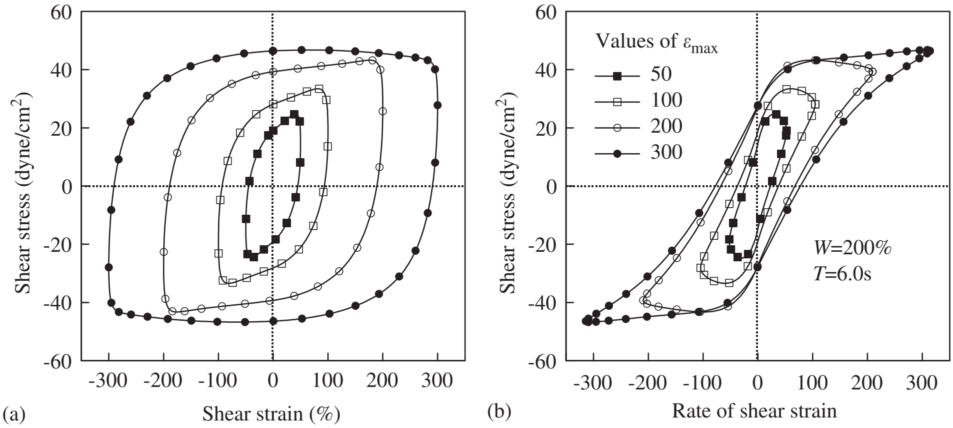

Fig. 1. Shear stress vs. shear strain (a) and rate of shear strain (b).

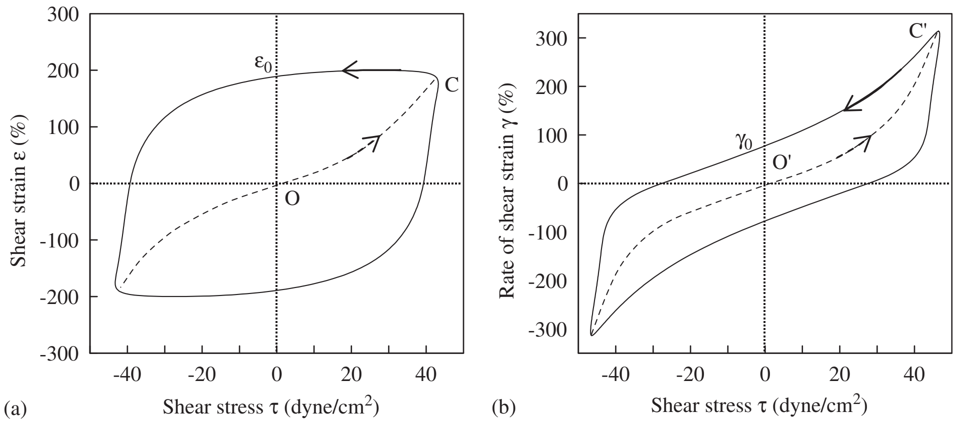

Fig. 2. Definition sketch illustrating the hysteresis phenomenon of mud.

if the strain is large enough, the stress-strain path will follow a large hysteresis loop resulting in higher energy dissipation. We give Fig. 2(a) and (b) as a definition sketch showing the hysteresis phenomenon of mud. Fig. 2(a) is of the shear strain versus shear stress, and Fig. 2(b) of the rate of shear strain versus shear stress. Note that, as dependent variables, the shear strain as well as the rate of shear strain are defined in the vertical coordinates. The imaginary lines $OC$and $O'C'$ in the figures are the initial curves illustrating relationships of the shear strain versus the shear stress and the rate of shear strain versus the shear stress at the beginning stage. When the shear stress due to oscillatory external forces decreases to zero, however, both the shear strain and the rate of shear strain do not return to zero along their initial curves OC and $O'C'$. This shows the shear strain as well as the rate of shear strain lag behind the shear stress. This is the hysteresis phenomenon of mud under external cyclic loadings. When the shear stress equals zero, the shear strain as well as the rate of shear strain do not equal zero, but ε_0 and γ_0, respectively, that is, a residue of the shear strain, and a residue of the rate of shear strain in the mud.

3. Governing equations of mud motion

Fig. 3 is a definition sketch of the water–mud model in which the water waves propagate in the x-direction. The surface and the inter-surface displacement are denoted by η and η_m, respectively; the thickness of the overlying water layer and the underlying mud layer by d_w and d_m, respectively. In the present study, the water layer will be treated as the Newtonian fluid and the mud layer will be treated as rheological materials of the constitution equation, Eq. (1). For both layers, the Navier–Stokes equations are given neglecting nonlinear terms:

$$\frac{\partial u}{\partial t} = -\frac{1}{\rho}\frac{\partial p}{\partial x} + \frac{1}{\rho}\frac{\partial \tau_{zx}}{\partial z}, \tag{6}$$

$$\frac{\partial w}{\partial t} = -\frac{1}{\rho}\frac{\partial p}{\partial z} + \frac{1}{\rho}\frac{\partial \tau_{xz}}{\partial x}, \tag{7}$$

$$\frac{\partial u}{\partial x} + \frac{\partial w}{\partial z} = 0 \tag{8}$$

in which p is the dynamic pressure, u and w are the velocity components in the horizontal (x) and vertical (z) direction, and ρ is the density.

For the mud layer, the shear stresses τ_{xz} and τ_{zx} in the above equations can be expressed in terms of velocities u and w by substituting shear strain ε and the rate of

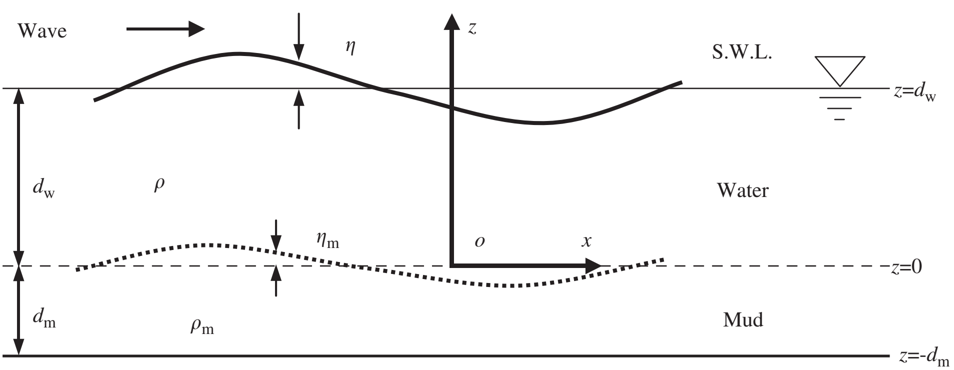

Fig. 3. Sketch of the two-layer water-mud model.

shear strain γ into the rheological model equation (1)

$$\varepsilon = \frac{\partial \xi}{\partial z} + \frac{\partial \zeta}{\partial x}; \ \gamma = \frac{\partial u}{\partial z} + \frac{\partial w}{\partial x}, \tag{9a,b}$$

where ξ and ζ are the components of the mud particle displacement in the horizontal (x) and vertical (z) directions, and

$$\xi = \int_0^t u \, dt; \ \varsigma = \int_0^t w \, dt. \tag{10a,b}$$

Eqs. (6)–(8) become a closed set of governing equations for the variables u, w and p. Here the solution is assumed to be

$$\begin{gathered} u(x,z,t) = \tilde{u}(z)e^{i(nx-\sigma t)}; \ w(x,z,t) = \tilde{w}(z)e^{i(nx-\sigma t)}; \\ p(x,z,t) = \tilde{p}(z)e^{i(nx-\sigma t)}; \ \eta(x,t) = ae^{i(nx-\sigma t)}, \end{gathered} \tag{11a–d}$$

where n is the complex wave number expressed by $n = n_r + i\delta$, whose real part n_r gives the wavelength ($2\pi/n_r$) and imaginary part δ gives the wave attenuation rate; η denotes the displacements of water surface and the intersurface; a is the amplitude.

Eq. (11) is incorporated into Eqs. (6)–(8). From Eq. (8), we have

$$\tilde{u} = \frac{i}{n}\frac{\partial \tilde{w}}{\partial z}. \tag{12}$$

Introduction of Eq. (12) into Eq. (6) yields

$$\tilde{p} = \frac{\rho_l v_l}{n^2}\frac{\partial^3 \tilde{w}}{\partial z^3} + \frac{\rho_l}{n^2}\frac{\partial v_l}{\partial z}\frac{\partial^2 \tilde{w}}{\partial z^2} + \left(\frac{i\rho_l \sigma}{n^2} - \rho_l v_l\right)\frac{\partial \tilde{w}}{\partial z}, \tag{13}$$

where subscript $l = 1$ or 2. $l = 1$ indicates the water layer, and v_1 is the viscosity of water; $l = 2$ denotes the mud layer, and v_2 is the viscosity of mud.

Substitution of $\tilde{p}$ into Eq. (7) yields the differential equation of the fourth order for $\tilde{w}$

$$\frac{\partial^4 \tilde{w}}{\partial z^4} + \frac{1}{v_l}\frac{\partial v_l}{\partial z}\frac{\partial^3 \tilde{w}}{\partial z^3} + \left[-2n^2 + \frac{n^2}{v_l}\left(\frac{\partial^2 v_l}{\partial z^2} + i\sigma\right)\right]\frac{\partial^2 \tilde{w}}{\partial z^2} - \frac{2n^2}{v_l}\frac{\partial v_l}{\partial z}\frac{\partial \tilde{w}}{\partial z} + \left(n^4 - \frac{in^2\sigma}{v_l}\right)\tilde{w} = 0. \tag{14}$$

The unsolved unknowns including the unknown variables n and a are determined by use of the following boundary conditions.

4. Boundary and initial conditions

For the vertical 2-D problem concerned in this study, the boundary conditions are given as follows:

At the water surface:

$$-p + 2\rho v_t \frac{\partial w}{\partial z} + \rho g \eta = 0; \ \rho v_t\left(\frac{\partial u}{\partial z} + \frac{\partial w}{\partial x}\right) = 0; \ \frac{\partial \eta}{\partial t} = w. \tag{15a–c}$$

At the water–mud inter-surface (the subscript w *denotes water layer, and* m *mud layer)*:

$$u_{\mathrm{w}} = u_{\mathrm{m}};\ \ w_{\mathrm{w}} = w_{\mathrm{m}};\ \ -p_{\mathrm{w}} + 2\rho v_t \frac{\partial w_{\mathrm{w}}}{\partial z} + \rho g \eta_{\mathrm{m}} = -p_{\mathrm{m}} + 2\rho_{\mathrm{m}} v_e \frac{\partial w_{\mathrm{m}}}{\partial z} + \rho_{\mathrm{m}} g \eta_{\mathrm{m}};$$
$$\rho v_t \left(\frac{\partial u_{\mathrm{w}}}{\partial z} + \frac{\partial w_{\mathrm{w}}}{\partial x} \right) = \rho_{\mathrm{m}} v_e \left(\frac{\partial u_{\mathrm{m}}}{\partial z} + \frac{\partial w_{\mathrm{m}}}{\partial x} \right);\ \ \frac{\partial \eta_{\mathrm{m}}}{\partial t} = w_{\mathrm{m}}. \tag{16a−e}$$

At the bottom:

$$u_{\mathrm{m}} = 0; \quad w_{\mathrm{m}} = 0. \tag{17a,b}$$

The initial condition is easily given by supposing that the calculation is started from static state.

5. Mud mass transport velocity

Under the action of water waves, the soft bottom mud may be forced into oscillatory motion. As a result, a positive mean velocity of a soft mud particle averaged over one wave period is induced. This phenomenon is the so-called mud mass transport, and the mean velocity of a soft mud particle is termed as the mud mass transport velocity.

The mud mass transport velocity can be evaluated by the following equation:

$$U_{\mathrm{L}} = U_{\mathrm{E}} + \overline{\frac{\partial u_{\mathrm{m}}}{\partial x} \int_0^t u_{\mathrm{m}}\,\mathrm{d}t} + \overline{\frac{\partial u_{\mathrm{m}}}{\partial z} \int_0^t w_{\mathrm{m}}\,\mathrm{d}t}, \tag{18}$$

where subscripts L and E denote the Lagrangian and Eulerian coordinates, respectively.

The sum of the second and the third terms on the right-hand side of Eq. (16) is known as Stokes's drift, and denoted by U_{S}.

The physical meaning of Stokes's drift can be explained as follows. In the Eulerian space coordinates, the velocity of a fluid particle at the top of the elliptic orbit is slightly larger than that at the bottom. Although this difference is not so large, the orbital path is not closed after one wave period. As a result, the fluid particle moves on the wave propagating direction.

On the other hand, the first term U_{E} in the right-hand side of Eq. (16) represents the mean Eulerian velocity, which exists due to the viscocity of the soft mud. By neglecting effect of the mean dynamic pressure, Sakakiyama and Bijker (1989) suggested a simple method for evaluating the value of U_E. The simplified equation takes the following form:

$$\mu_{\mathrm{m}} \frac{\partial^2 U_{\mathrm{E}}}{\partial z^2} = \frac{\partial(\rho_{\mathrm{m}}\ \overline{u_{\mathrm{m}}^2})}{\partial x} + \frac{\partial(\rho_{\mathrm{m}}\ \overline{u_{\mathrm{m}} w_{\mathrm{m}}})}{\partial z}, \tag{19}$$

where μ_{m} denotes the viscosity of the Newtonian fluid, which is a constant.

Thus, the mean Eulerian velocity can be evaluated from Eq. (19) under the following boundary conditions:

$$U_{\mathrm{E}}|_{z=-d_{\mathrm{m}}} = 0;\ \ = \frac{\partial U_{\mathrm{E}}}{\partial z}|_{z=0} = 0. \tag{20a,b}$$

Consequently, the mud mass transport velocity can be calculated by the sum of the Stokes's drift U_S and the mean Eulerian velocity U_E.

6. Verifications of the numerical model

The finite difference method is applied to the numerical implementation. A logarithm grid is used for both sides of the water–mud inter-surface. Numerical experiments were conducted to examine the general performance of the developed numerical model for simulating the wave-induced mud motion, the resultant mud mass transport as well as surface wave attenuation. A view of the calculated result for the whole computational domain is shown in Fig. 4, in which the water wave surface damping along the wave propagating direction is easily seen, and the wave-induced mud motion is characterized by the features of laminar flow, in which mud particles move in oscillatory form in response to the wave action. Part of the vector field of velocity in the neighborhood of the water–mud inter-surface is shown in Fig. 5. Profiles of the horizontal velocity for different mud density along the full depth are shown in Fig. 6. Here, depth of the mud layer is 0.10 m for both of the above figures. These figures show that the logarithm grid treatment can give a description of the flow structures, particularly in the neighborhood of the water–mud inter-surface. Meanwhile, features of the calculated distribution of velocity along mud depth reflect a noticeable phase lag due to strong nonlinearity in the mud rheological behavior.

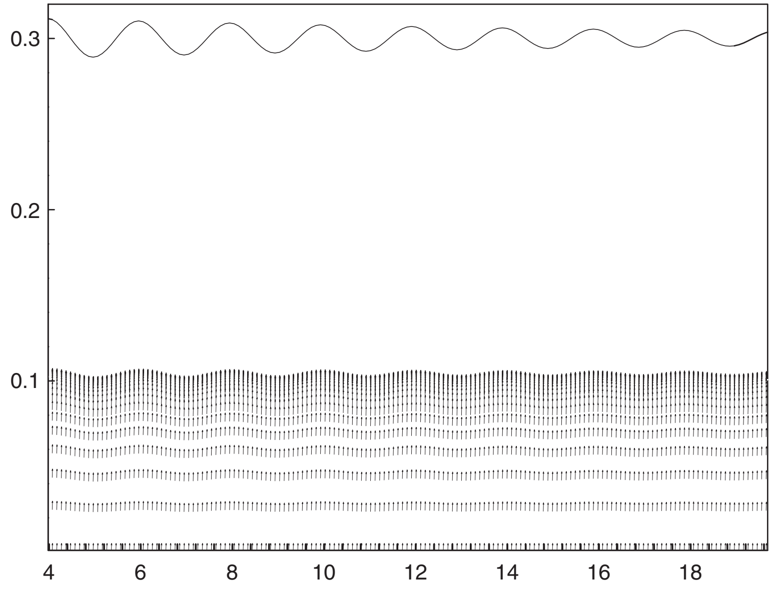

Fig. 4. A view of the calculated result for the whole computational domain (from 4 to 19.8 m).

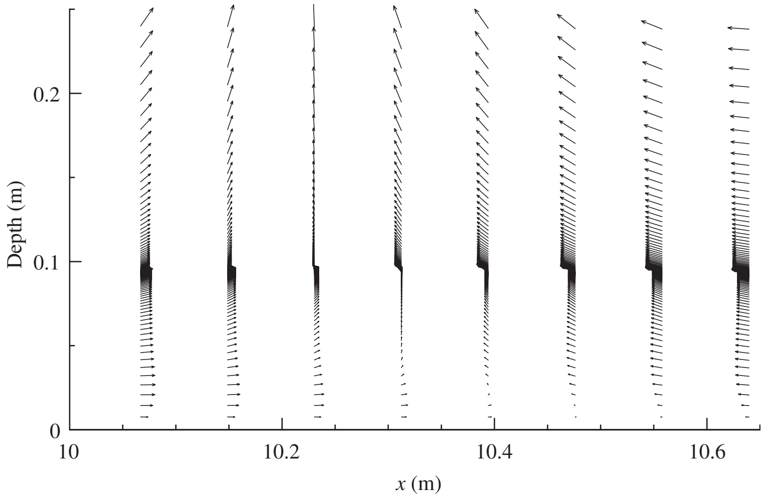

Fig. 5. Velocity field in the water and mud layers using logarithm grid.

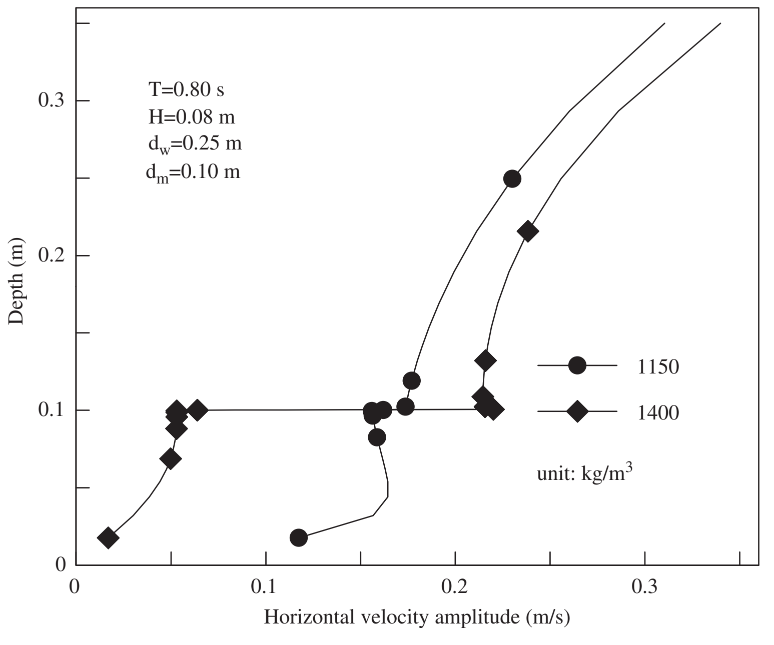

Fig. 6. Profiles of horizontal velocity amplitude using logarithm grid.

In order to verify the numerical model for simulating surface waves attenuation due to soft mud beds, the calculated rate of decay of surface wave height is first compared with the experimental data by Lian (1993).

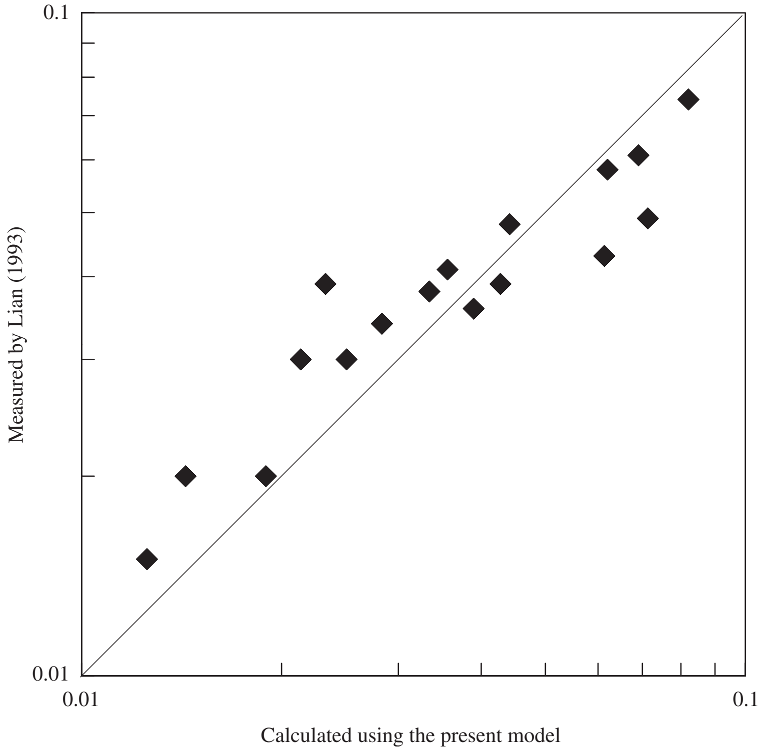

Fig. 7. Comparison between the calculated and measured rate of decay of surface wave height.

Fig. 7 shows the comparison between the calculated and measured rate of decay of surface wave height. It can be seen that the calculated and measured results are in good agreement.

Define parameter $\tilde{d}$ as the ratio of the mud layer thickness d_{m} to the Stokes's boundary layer thickness δ_{m}:

$$\tilde{d} = d_{\mathrm{m}}/\delta_{\mathrm{m}}, \tag{21}$$

$$\delta_m \equiv \left(2v_m/\sigma\right)^{\frac{1}{2}}, \tag{22}$$

where v_m is defined as the depth-averaged mud viscosity, and

$$v_{\mathrm{m}} \equiv \frac{1}{d_{\mathrm{m}}}\int_0^{d_{\mathrm{m}}} v_e(z)\,\mathrm{d}z. \tag{23}$$

The dimensionless parameter $\tilde{d}$ was applied in the study of the rate of decay of surface wave height. Fig. 8 shows the numerical results of the rate of decay of surface wave height as a function of the dimensionless parameter $\tilde{d}$. It can be easily seen that the most pronounced wave damping occurs when the mud thickness is 1.2–1.5 times

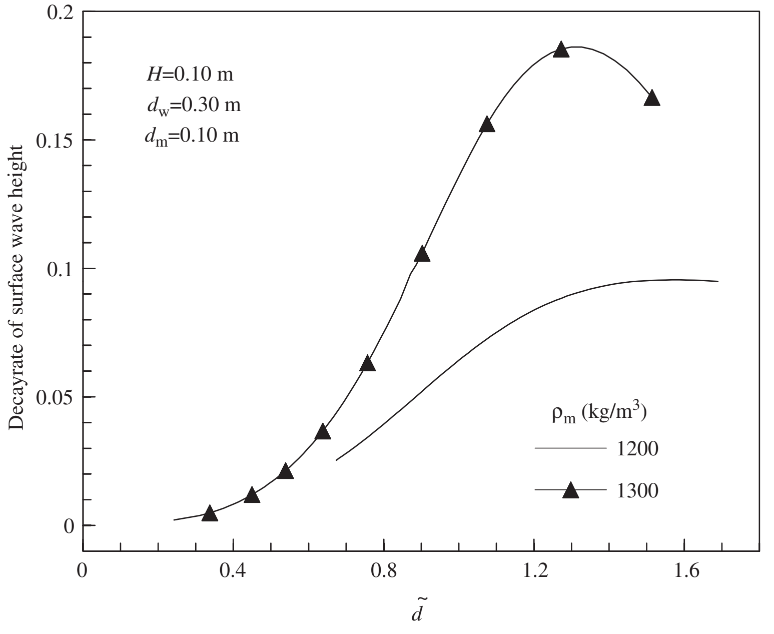

Fig. 8. Rate of decay of wave height as a function of $\tilde{d}$.

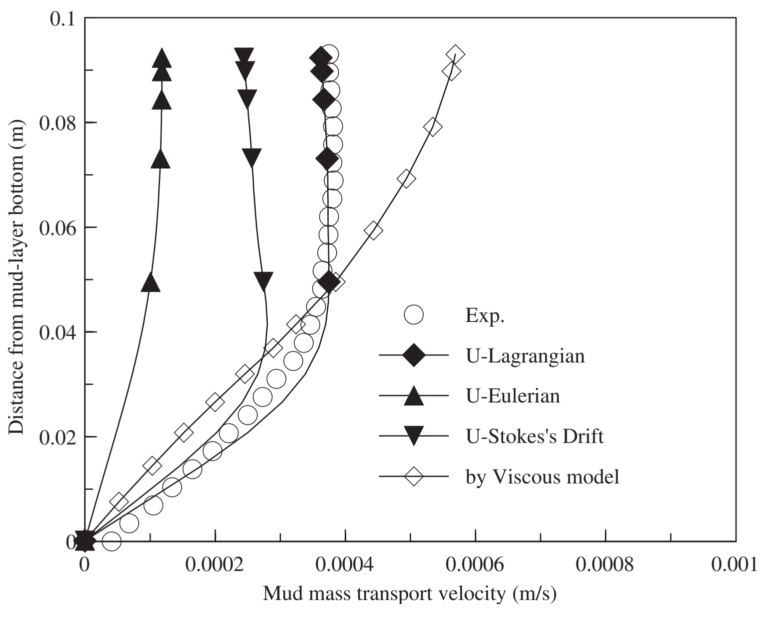

Fig. 9. Measured and calculated profiles of mud mass transport velocity.

the Stokes' boundary layer thickness of mud, in other words, when the mud layer is 20–50% thicker than the boundary layer. This is in good agreement with Dalrymple and Liu (1978) and Ng (2000) (in Dalrymple and Liu (1978), $\tilde{d} = 1.3$–1.5; in Ng (2000), $\tilde{d} = 1.5$).

On the other hand, in order to verify the present model for simulating mud mass transport velocity due to surface waves, the calculated results are compared with the experimental data by Sakakiyama and Bijker (1989). These measured data were obtained under the homogeneous mud bed by using the mixture of commercial kaolinite and tap water and the technique for measuring mud mass transport was confirmed reliable by Huynh (1991) and Shen et al. (1993). For case study, values of the parameters concerned in the numerical simulation are given as in Sakakiyama and Bijker (1989), that is, density of the homogeneous mud is 1300 kg/m^3; the incident water wave height and period are 0.027 m and 1.01 s, respectively; depth of the water layer and the mud layer are 0.3 and 0.093 m, respectively. Fig. 9 compares the calculated and measured mud mass transport velocity of homogeneous soft mud. It is easily seen that the calculated and measured profiles of the Lagrangian transport velocity agree very well, and in particular, for the flow in the upper part of the mud layer, good resolution and accuracy are achieved due to the logarithmic grid in the vertical direction. The present model is much better than viscous model as well as than Shen et al. (1993) and Jiang (1996) in the prediction of mud mass transport velocity, the agreement between the calculation and the measurement is satisfactory.

7. Concluding remarks

A vertical 2-D two-layer numerical model has been developed for simulating the interaction between water waves and the underlying soft mud bed and is featured by: (a) the strong nonlinearity and hysteresis characteristics of the rheological properties of soft mud is taken into account and (b) the use of logarithmic grid for the both sides of the water–mud inter-surface in the vertical direction. The main conclusions drawn from this study are as follows:

The rheological properties of soft mud are strongly nonlinear with characteristics of remarkable hysteresis phenomenon under external cyclic loadings in the relationships of the shear stress versus both the shear strain and the rate of shear strain of mud. That is, when the shear stress decreases to zero, the shear strain as well as the rate of shear strain do not return to zero, but a residue of the shear strain as well as a residue of the rate of shear strain left in the mud.

The logarithmic grid technique proves to be helpful to the resolution of flow in the neighborhood of the water–mud inter-surface.

The 2-D numerical model of mud motion under water waves on the basis of the semi-empirical rheology model has been developed to predict the wave attenuation as well as the bed mud motion. Agreement between the calculation and laboratory data of Lian (1993) and Sakakiyama and Bijker (1989) is good for the rate of decay of surface wave height and satisfactory for the mud mass transport velocity.

However, the present study on the problems of the interaction between water waves and soft mud bed is just a step towards fully understanding of the phenomena. Many subjects and much work are left to the future study. These include, for instance, the flocculation, settling, deposition and erosion of cohesive sediment, the fluidization and liquefaction of mud bed layers, as well as the motion of bed mud under both waves and currents.

References

Dalrymple, R.A., Liu, P.L-F., 1978. Waves over soft mud: a two-layer fluid model. Journal of Physical Oceanography 8, 1121–1131.

Dawson, T.H., 1978. Wave propagation over a deformable sea floor. Ocean Engineering 5, 227–234.

Gade, H.G., 1958. Effects of a non-rigid impermeable bottom on plane surface waves in shallow water. Journal of Marine Research 16, 61–82.

Hsiao, S.V., Shemdin, O.H., 1980. Interaction of ocean waves with a soft bottom. Journal of Physical Oceanography 10, 605–610.

Huynh, T. N., 1991. Study on mud transport in coastal waters. Ph.D. Thesis, University of Tokyo, Japan.

Jiang, Q., 1996. Study on rheological properties and mass transport of soft mud under water waves. Ph.D. Thesis, University of Tokyo, Japan.

Kihara, T., Takahashi, M., Matsumoto, M., et al., 1987. Observation of silt transport in shallows, In: Proceedings of the 34th Japanese Conference on Coastal Engineering vol: 34, 397–401, (in Japanese).

Kraft, L. M., Watkins, D. J., 1976. Prediction of wave-induced seafloor movements. In: Proceedings of the 15th Conference on Coastal Engineering, ASCE, New york, pp. 1605–1623.

Krone, R.B., 1963. A study of rheological properties of estuarine sediments. Technical Bulletin No. 7, Committee on Tidal Hydraulics. US Army Corps of Engineers, Waterways Experiment Station, Vicksburg, USA.

Lian, J., 1993. Interactions among waves, currents and muddy bottoms. Ph.D. Thesis, Tianjin University, China (in Chinese).

Maa, J.P.-Y., Mehta, A.J., 1990. Soft mud response to water waves. Journal of Waterway, Port, Coastal and Ocean Engineering—ASCE 116 (5), 634–650.

Macpherson, H., 1980. The attenuation of water waves over a non-rigid bed. Journal of Fluid Mechanics 97, 721–742.

Mallard, W. W., Dalrymple, R. A., 1977. Water waves propagating over a deformable bottom. In: Proceedings of the ninth Conference on Offshore Technology, pp. 141–146.

Mei, C.C., Liu, K-F., 1987. A Bingham plastic model for a muddy seabed under long waves. Journal of Geophysical Research 92 (C13), 14581–14594.

Ng, C.O., 2000. Water waves over a muddy bed: a two-layer Stokes' boundary layer model. Coastal Engineering 40, 221–242.

Sakakiyama, T., Bijker, E.W., 1989. Mass transport velocity in mud layer due to progressive waves. Journal of Waterway, Port, Coastal and Ocean Engineering—ASCE 115 (5), 614–633.

Shen, D., Isobe, M., Watanabe, A., 1993. Mud mass transport under waves based on an empirical rheology model. In: Proceedings of the 25th IAHR Congress, No. C-4-2, pp. 120–127.

Shibayama, T., Okuno, M., Sato, S., 1990. Mud transport rate in mud layer due to wave action. In: Proceedings of the 22nd Conference on Coastal Engineering, ASCE, pp. 3037–3048.

Trien, H. N., 1991. Study on mud transport in coastal waters. Ph.D. Thesis, University of Tokyo, Japan.

Trien, H.N., Isobe, M., Kobayashi, T., et al., 1990. An experimental study on rheological properties of mud in the coastal waters. Proc Coastal Engineering—JSCE 37, 225–229 (in Japanese).

Yamamoto, T., Takahashi, S., 1985. Wave damping by soil motion. Journal of Waterway Port, Coastal and Ocean Engineering—ASCE 111 (1), 62–77.